

# Trimming the UCERF3-TD Logic Tree: Model Order Reduction for an Earthquake Rupture Forecast Considering Loss Exceedance

Keith Porter,<sup>a)</sup> M.EERI, Kevin Milner,<sup>b)</sup> and Edward Field<sup>c)</sup> M.EERI

The Uniform California Earthquake Rupture Forecast version 3-Time Dependent depicts California's seismic faults and their activity. Its logic tree has 5,760 leaves. Considering 30 more model combinations related to ground motion produces 172,800 distinct models representing so-called epistemic uncertainties. To calculate risk to a portfolio of buildings, one also considers millions of earthquakes and spatially correlated ground-motion variability. We offer a tree-trimming technique that retains the probability distribution of portfolio loss. We applied it to a California statewide building portfolio and various levels of nonexceedance probability between 1 in 100 and 1 in 2,500. We trimmed the logic tree from 172,800 leaves to as few as 15. The result: a supercomputer that would otherwise run 24 hours to estimate the distribution of 1-in-250-year loss can calculate it in moments with the reduced-order model. Others can use the reduced-order model to calculate risk to different California portfolios, and scientists can prioritize study to reduce the remaining epistemic uncertainty.

## INTRODUCTION

*Why the size of the UCERF3-TD logic tree matters.* The Uniform California Earthquake Rupture Forecast version 3-Time Dependent (UCERF3-TD, Field et al. 2015) mathematically models seismic activity in California. UCERF3-TD can be represented using a logic tree with eight modeling choices—branches in the logic tree—often called epistemic uncertainties. Branches have as few as two and as many as five discrete possible values. The choices allow for 5,760 combinations. Counting three more logic-tree branches for aspects of ground motion prediction, UCERF3-TD with a full ground-shaking model has 172,800 combinations of 11

---

<sup>a)</sup> Institute for Catastrophic Loss Reduction, 800 Collip Cir, London ON N6G 4M3, Canada, kporter@iclr.org

<sup>b)</sup> Southern California Earthquake Center, 3651 Trousdale Pkwy Rm 169, Los Angeles CA 90089

<sup>c)</sup> U.S. Geological Survey, 1711 Illinois St, Golden, CO 80401

27 model elements. One must choose one option for each model element before one can calculate  
28 loss in a single earthquake. Each set of choices can produce a different value of loss.

29 With 172,800 choices, each with an associated probability of being the right choice and  
30 each capable of giving a different answer, the loss takes on a probability distribution. Its range  
31 of possible values spans an order of magnitude, i.e., a multiplicative error of 3 or more either  
32 way. Multiply by the so-called aleatory uncertainties of the between-events ground-motion  
33 variability, spatially correlated within-event ground-motion variability, and approximately  
34 6,000,000 possible earthquake ruptures, and one can glimpse how robust calculation of the risk  
35 to a large portfolio of properties can grow prohibitively computationally expensive for anyone  
36 without access to a supercomputer. How large can a portfolio get? We estimate that the state  
37 of California has on the order of 10 million buildings.

38 State policymakers and insurance executives might want to know the monetary loss or  
39 number of fatalities with some specified rare but inevitable likelihood, such as the loss with 1  
40 chance in 500 of happening next year. Few people have the resources to calculate the  
41 probability distribution of loss without making simplifying assumptions that might lead to a  
42 gross over- or under-estimate of the value with 0.2% chance of happening next year.

43 Some decision-makers can tolerate an answer that could be low or high by a factor of 3,  
44 but many cannot. Large insurers must buy reinsurance to be confident that a rare earthquake  
45 has a low chance of bankrupting them. Reinsurance can represent half of an insurer's annual  
46 budget (California Earthquake Authority 2022). If they buy 1/3rd as much as they need, they  
47 risk ruining themselves and their insureds through their inability to pay claims. If they buy  
48 three times too much, they must double the premiums they charge policyholders, which merely  
49 accelerates their bankruptcy when insureds cancel their policies. To make the right choice with  
50 confidence requires knowing the probability distribution of loss.

51 In two prior works that we discuss later, we offer new methods for trimming an earthquake  
52 rupture forecast logic tree to reduce computational effort without reducing uncertainty or  
53 biasing an estimate of expected annualized loss. In the present work, we revisit those methods  
54 with a similar goal, but considering large, rare losses rather than average annualized losses.

55 **Objectives.** The branches of the logic tree contribute unequally to loss uncertainty. Some  
56 contribute greatly to uncertainty, some do not. If one can find out which is which, one can fix  
57 the less-important modeling choices to a single value. If one can eliminate a branch with three

58 choices, one reduces the size of the model by 3 times. Fix two logic-tree branches and the  
59 problem gets smaller by 9 times, requiring  $1/9^{\text{th}}$  the computational effort. Fix another and the  
60 problem is smaller by 27 times, requiring only 4% of the computational effort as before.

61 Mathematicians call that process “model order reduction.” Refer to Schilders et al. (2008)  
62 for general treatment. The goal of model order reduction is to find and fix as many branches of  
63 the logic tree as possible without changing the probability distribution of loss. Mathematicians  
64 have developed a rich body of model order reduction techniques. Most of them only work with  
65 scalar random variables, i.e., one-dimensional numbers that have scale such as the maximum  
66 earthquake magnitude that can occur away from a mapped fault. But between UCERF3-TD’s  
67 native earthquake-rupture branches and the additional ground-motion model elements, 7 of 11  
68 logic-tree branches for a statewide risk calculation are nominal random variables.

69 A nominal random variable can take on values with no scale or order, no average, no  
70 standard deviation. For example, in one branch of UCERF3-TD, one chooses between five  
71 models of the relationship among slip length, rupture area, and magnitude. Each model  
72 corresponds to a different scholarly article. One chooses between the five articles. There is no  
73 sense in which the articles have a meaningful order or scale. Most existing model-order-  
74 reduction techniques do not apply to models with nominal random variables.

75 Here, we seek to select a single option for as many branches of UCERF3-TD plus the added  
76 ground motion uncertainties as we can, without changing the probability distribution of  
77 statewide portfolio loss each year with 1 chance in 100, 1 in 250, 1 in 400, 1 in 550, and 1 in  
78 2,500. How does doing so help anyone? Our goals are twofold:

79 (1) Make the calculation of portfolio loss easier for other people who have different portfolios  
80 and no supercomputer. If they can ignore some branches, they can perform robust risk  
81 calculations that would otherwise take too long. That is, we aim to find a subset of logic  
82 tree branches in the present work that other people can use in their loss estimates so that  
83 they do not have to model all the logic tree branches of UCERF3-TD.

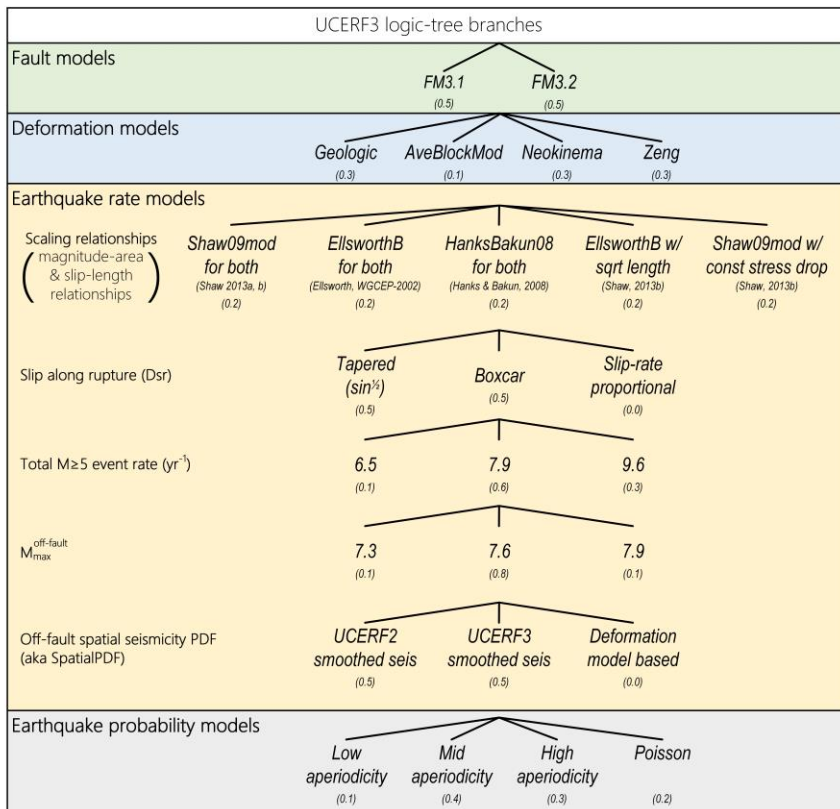
84 (2) Find the UCERF3-TD model variables that contribute most to uncertainty. Further study  
85 of those branches might yield new knowledge and reduce epistemic uncertainty.

86 Although we apply our solution to UCERF3-TD, it could apply to other problems: to future  
87 California earthquake hazard risk models, to earthquake models outside of California, to

88 catastrophe risk models for other perils, and perhaps to other models with a mixture of nominal  
 89 and scalar random variables.

90 **LITERATURE REVIEW**

91 **UCERF3-TD logic tree.** Let us first review the UCERF3-TD logic tree, then review model  
 92 order reduction techniques. Field et al. (2013) offer a new earthquake rupture forecast for  
 93 California: the Uniform California Earthquake Rupture Forecast version 3, Time-Independent,  
 94 or UCERF3-TI. It has seven uncertain model components arranged in a logic tree. Each branch  
 95 has two to five choices, each with a weight (a degree of belief or Bayesian probability). Field  
 96 et al. (2015) add an eighth element to model aperiodicity in earthquake recurrence that makes  
 97 the model time-dependent (hence the name Uniform California Earthquake Rupture Forecast  
 98 version 3, Time-Dependent, or UCERF3-TD). Refer to Figure 1. Of the eight uncertain  
 99 parameters, only three are scalar: total event rate of earthquakes of magnitude 5 or greater,  
 100 maximum off-fault magnitude, and aperiodicity. We detail UCERF3-TD later.



101  
 102 **Figure 1.** UCERF3-TD logic tree. Each branching point represents an uncertain variable; each branch  
 103 a possible value.

104 **Model order reduction techniques.** Size limitations prevent a thorough review of model  
 105 order reduction techniques, but a summary seems useful. They fall into five classes: proper

106 orthogonal decomposition, reduced bias, simplified physics, nonlinear dimensionality  
107 reduction, and balancing methods. Proper orthogonal decomposition (e.g., Loeve 1955)  
108 requires one to evaluate and operate on a covariance matrix and find a smaller number of  
109 eigenvalues and eigenvectors, essentially changing  $n$  potentially correlated random variables  
110 into fewer than  $n$  uncorrelated ones. But there is no such thing as a correlation matrix for  
111 nominal random variables. The reduced-bias technique (e.g., Prud'homme et al. 2002) operates  
112 on linear functions of elliptic and parabolic partial differential equations; again, only scalar  
113 variables. A simplified-physics approach replaces a complex model with a simpler one using  
114 physical insight or empirical observation, which seems unhelpful to choosing between the  
115 modeling options considered here, which are already physically based and empirically  
116 supported. Balancing methods involve diagonalization of positive definite matrices (e.g.,  
117 Antoulas 2005), again a problem limited to scalar values. Some nonlinear dimensionality  
118 reduction techniques might accommodate nominal variables: Graeme Weatherill (GFZ  
119 German Research Centre for Geosciences, written commun., November 8, 2023) suggests that  
120 t-distributed stochastic neighbor embedding (t-SNE) and uniform manifold approximation and  
121 projection (UMAP) could accommodate nominal variables. One can encode the nominal  
122 dimensions numerically such as with binary variables representing each category. Refer to e.g.,  
123 McInnes et al. (2020) appendix C and Awan (2023). These methods might work, but the one  
124 we have in mind seems simpler, at least to us, and we know it works with OpenSHA (Field et  
125 al 2005), the software that encodes UCERF3-TD.

126 To reduce the computational expense of UCERF3-TD, some authors have replaced the  
127 earthquake rupture forecast with a Monte Carlo time series called an event set. That is, one  
128 creates a sequence of scenario earthquakes spread over thousands of years or more, consistent  
129 with the earthquake rupture forecast. For example, Perkins and Taylor (2003) use a 50,000-  
130 year event set to estimate risk to a roadway system. They find the effort highly computationally  
131 demanding and attempt a variety of model order reduction techniques, including bootstrap  
132 sampling, the use of antithetic variates, the use of Latin Squares (or permutation) sampling, the  
133 use of control functions, a compound Poisson approach, and importance sampling. They  
134 achieved large reductions in the required number of simulations for the mean and confidence  
135 limits of the conditional loss distribution (the loss distribution given some loss in a specific  
136 year), but only a threefold reduction for the unconditional, annual-loss distribution.

137 Kotha et al. (2018) offer a method to select an event set by matching the mean hazard at  
138 selected locations. Using six small portfolios of buildings in the San Francisco Bay Area, they  
139 show that they can reasonably reproduce average annualized losses and the loss exceedance  
140 curves generated by a catalog that represents a reduced version of the UCERF2 earthquake  
141 rupture forecast (Field et al. 2007). Event sets can reduce computational effort, but they shed  
142 no light on which branches of the logic tree matter to the distribution of loss, a central objective  
143 of the present work.

144 In prior work (Porter et al. 2012) we applied a deterministic sensitivity analysis technique  
145 called tornado-diagram analysis meant to identify the important variables in UCERF2 (Field  
146 et al. 2007). In Porter et al. (2017), we offer new a model order reduction technique that works  
147 on models with nominal random variables. We applied it to UCERF3-TD, using the expected  
148 annualized loss, *EAL*, to a proxy for the California Earthquake Authority’s (CEA) statewide  
149 insurance portfolio. (*EAL* measured ground-up repair cost rather than insured loss after  
150 deductibles and limits.) We found a reduced-order model that required evaluating 60 leaves  
151 out of 57,600. Why not 172,800? Because in that work, we ignored a variable called added  
152 epistemic uncertainty recommended by Atik and Youngs (2014).

## 153 METHODOLOGY

154 *Evaluate the model output for one logic-tree leaf.* One begins by selecting an asset  
155 portfolio and evaluating the portfolio loss exceedance curve for one logic-tree leaf. That is, fix  
156 every branch to one value and evaluate loss in each rupture in the UCERF3-TD model.  
157 Calculate the loss exceedance curve as follows. Let

158  $N_a$  = number of assets in the portfolio

159  $a$  = an index to assets in the portfolio,  $a \in \{0, 1, \dots, N_a - 1\}$

160  $V_a$  = replacement cost of asset  $a$

161  $V$  = replacement cost of the portfolio; refer to equation (1)

$$162 \quad V = \sum_{a=0}^{N_a-1} V_a \quad (1)$$

163  $N_k$  = number of possible ruptures among full UCERF3-TD model

164  $k$  = an index to scenario ruptures (“ruptures”),  $k \in \{0, 1, \dots, N_k - 1\}$

165  $X_{a/k}$  = uncertain ground motion at asset  $a$  given rupture  $k$

166  $x$  = ground motion, e.g., 5% damaged elastic spectral acceleration response at 1.0 sec period  
 167  $f_{X_{a/k}}(x)$  = probability density function of  $X_{a/k}$ , evaluated at  $x$ , given by the ground-motion-  
 168 prediction equation, as in equation (2), in which  $\phi$  denotes the Gaussian probability density  
 169 function. Ground-motion-prediction equations generally assume lognormally distributed  
 170 ground motion conditioned on rupture and site parameters, and provide a median and  
 171 logarithmic standard deviation, denoted here by  $\theta_{x_a}$  and  $\beta_{x_a}$ .

$$172 \quad f_{X_{a/k}}(x) = \phi\left(\frac{\ln(x/\theta_{x_a})}{\beta_{x_a}}\right) \quad (2)$$

173  $y_a(x)$  = mean repair cost as a fraction of replacement cost for asset  $a$ , given ground motion  $x$ .  
 174 This quantity is evaluated using a vulnerability function (e.g., Porter 2009a, b, and 2010).

175  $\mu_{L/k}$  = expected value of portfolio loss  $L$  given rupture  $k$ . For portfolios with assets that are  
 176 spaced less than a few kilometers apart, within-event spatial correlation of ground motion  
 177 matters. One can sample over  $N_\tau$  values of the between-event ground-motion variability  
 178 and  $N_f$  spatially correlated random fields of within-event ground-motion variability, and  
 179 apply equation (3). In the equation,  $i$  is an index to between-event values,  $j$  is an index to  
 180 stochastic simulations of within-event variability,  $x_{ai,j}$  is the ground motion at asset  $a$  given  
 181 between-event term  $i$  and within-event simulation  $j$ , and  $w_{\tau i}$  denotes the weight applied to  
 182 between-event value  $i$ . Refer to Porter et al. (2024) for details of the spatially correlated  
 183 ground motions and for a simplification to equation (3).

$$184 \quad \mu_{L/k} = \sum_{i=0}^{N_\tau-1} \sum_{j=0}^{N_f-1} \sum_{a=0}^{N_a-1} V_a y_a(x_{ai,j}) w_{\tau i} \frac{1}{N_f} \quad (3)$$

185  $L$  = uncertain portfolio loss

186  $l$  = a value of  $L$

187  $\delta_{L/k}$  = coefficient of variation of portfolio loss in rupture  $k$ . Refer to Porter et al. (2024) for a  
 188 method to estimate  $\delta_{L/k}$  as a function of  $\mu_{L/k}$ . As others have found for individual assets  
 189 (e.g., Porter 2010), portfolio loss uncertainty decreases with increasing portfolio loss, as in  
 190 the equation (4). In the equation, the coefficient  $1000/V$  normalizes the mean loss in terms  
 191 of loss per \$1000 of replacement cost, a loss measure sometimes used in the catastrophe-  
 192 risk modeling industry. Porter et al. (2024) presents a regression analysis that suggests the

193 following values for  $c_1$  and  $c_2$ . The resulting curve gradually drops from 2 (at low portfolio  
194 loss) to 0.5 (at high portfolio loss).

195  $c_1$  = a parameter for estimating  $\delta_{L/k} = 0.9832$

196  $c_2$  = a parameter for estimating  $\delta_{L/k} = -0.117$

$$197 \quad \delta_{L/k} \approx c_1 \cdot \left( \frac{1000}{V} \mu_{L/k} \right)^{c_2} \quad (4)$$

198  $\theta_{L/k}$  = median value of portfolio loss  $L$  given rupture  $k$ , assuming that  $L$  is approximately  
199 lognormally distributed; refer to equation (5). Porter et al. (2024) offers evidence.

$$200 \quad \theta_{L/k} = \frac{\mu_{L/k}}{\sqrt{1 + (\delta_{L/k})^2}} \quad (5)$$

201  $\beta_{L/k}$  = standard deviation of the natural logarithm of portfolio loss  $L$  given rupture  $k$ , assuming  
202 that  $L$  is approximately lognormally distributed. Refer to equation (6).

$$203 \quad \beta_{L/k} = \sqrt{\ln\left(1 + (\delta_{L/k})^2\right)} \quad (6)$$

204  $r_k$  = rate at which rupture  $k$  occurs, given the choice of logic tree leaf. The earthquake rupture  
205 forecast (e.g., Field et al. 2015) provides  $r_k$ . The reader may wonder how rate comes from  
206 a time-dependent model. Here,  $r_k$  is the equivalent Poisson rate implied by the chosen start  
207 date and duration of the forecast.

208  $G(l)$  = number of earthquakes per year producing  $L \geq l$ . The relationship between  $G(l)$  and  $l$  is  
209 often called the loss exceedance curve. By the theorem of total probability, the rate is the  
210 sum of event rates  $r_k$  times probability that the loss in rupture  $k$  is greater than or equal to  
211  $l$ , as shown in equation (7).

$$212 \quad G(l) = \sum_{k=0}^{N_k-1} r_k \cdot \left( 1 - \Phi \left( \frac{\ln(l/\theta_{L/k})}{\beta_{L/k}} \right) \right) \quad (7)$$

213  $L_p$  = loss with a specified exceedance rate, rather than the exceedance rate of some value of  
214 loss. It is the inverse of the loss exceedance curve evaluated at  $p$ , as shown in equation (8)

$$215 \quad L_p = G^{-1}(p) \quad (8)$$

216 ***Evaluate the cumulative distribution function of the full model output.*** Let

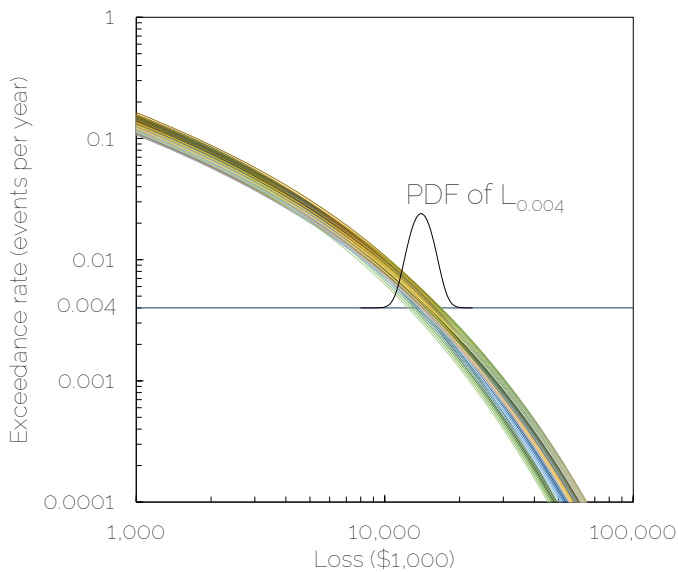
217  $Z$  = number of leaves in the original model



218  $j = \text{an index to leaves, } j \in \{0, 1, \dots, Z - 1\}$

219  $w_j = \text{weight of leaf } j \text{ in the full model. The earthquake rupture forecast (e.g., Field et al. 2015)}$   
220  $\text{specifies leaf weights.}$

221  $L_{p,j} = \text{loss associated with exceedance frequency } p \text{ in logic-tree leaf } j, \text{ from equation (8). Note}$   
222  $\text{that each leaf } j \text{ can have a different loss exceedance curve and therefore a different value}$   
223  $\text{of loss associated with exceedance frequency } p, \text{ and therefore a probability distribution of}$   
224  $L_p, \text{ as illustrated in Figure 2. The figure shows a suite of loss exceedance curves for many}$   
225  $\text{logic-tree leaves. It also shows a horizontal line at some exceedance rate } p \text{ of interest (0.004}$   
226  $\text{per year), and a probability density function of } L_p. \text{ The probability density function has}$   
227  $\text{some mean value that we could denote by } \mu_{L_p} \text{ and a coefficient of variation denoted by } \delta_{L_p}.$   
228  $\text{It will not be necessary to assume a parametric form of the distribution of } L_p \text{ such as normal}$   
229  $\text{or lognormal.}$



230

231 **Figure 2.** Illustration of the probability density function (PDF) of  $L_p$ . The colored curves represent loss-  
232 exceedance curves for different logic-tree leaves. The present model-order-reduction effort aims to  
233 reduce the number of possible loss exceedance curves (thereby simplifying the model and reducing  
234 computational effort) without strongly affecting the PDF of large, rare loss.

235  $F_{L_p}(l) = \text{cumulative distribution function for } L_p \text{ in the full model using equation (9), in which}$   
236  $H$  is the Heaviside function, as shown in equation (10).  $F_{L_p}(l)$  has a mean value given by  
237 equation (11), variance by equation (12), and coefficient of variation by equation (13).

238 
$$F_{L_p}(l) = \sum_{j=0}^{Z-1} w_j \cdot H(l - L_{p,j}) \quad (9)$$

239 
$$H(x) = \begin{cases} 0 & x < 0 \\ 0.5 & x = 0 \\ 1 & x > 0 \end{cases} \quad (10)$$

240 
$$\mu_{L_p} = \sum_{j=0}^{Z-1} L_{p,j} \cdot w_j \quad (11)$$

241 
$$\sigma_{L_p}^2 = \left( \sum_{j=0}^{Z-1} (L_{p,j})^2 \cdot w_j \right) - (\mu_{L_p})^2 \quad (12)$$

242 
$$\delta_{L_p} = \frac{\sigma_{L_p}}{\mu_{L_p}} \quad (13)$$

243 ***Evaluate the loss exceedance curve for a reduced-order model.*** Here is how to evaluate  
 244 the exceedance curve for a reduced model and to measure the error in loss with a specified  
 245 exceedance rate  $L_p$ .

246  $I_j$  is a binary indicator (1,0) whether a reduced model includes ( $I_j = 1$ ) or excludes ( $I_j = 0$ ) logic-  
 247 tree leaf  $j$

248  $z$  = model size of reduced model, meaning the number of leaves in it, by equation (14).

249 
$$z = \sum_{j=0}^{Z-1} I_j \quad (14)$$

250  $c_0$  = normalizing constant for weights in the reduced-order model, using equation (15).

251 
$$c_0 = \sum_{j=0}^{Z-1} w_j \cdot I_j \quad (15)$$

252 Now find the cumulative distribution function of  $L_p$  in the reduced model:

253  $\hat{F}_{L_p}(l)$  = cumulative distribution function for  $L_p$  in reduced model, by equation (16), which  
 254 has an expected value given by equation (17), variance given by equation (18), and  
 255 coefficient of variation given by equation (19).

256 
$$\hat{F}_{L_p}(l) = \frac{1}{c_0} \cdot \sum_{j=0}^{Z-1} w_j \cdot I_j \cdot H(l - L_{p,j}) \quad (16)$$

257 
$$\hat{\mu}_{L_p} = \frac{1}{c_0} \sum_{j=0}^{Z-1} L_{p,j} \cdot w_j \cdot I_j \quad (17)$$

258 
$$\hat{\sigma}_{L_p}^2 = \left( \frac{1}{c_0} \sum_{j=0}^{Z-1} (L_{p,j})^2 \cdot w_j \cdot I_j \right) - (\hat{\mu}_{L_p})^2 \quad (18)$$

259

$$\hat{\delta}_{L_p} = \frac{\hat{\sigma}_{L_p}}{\hat{\mu}_{L_p}} \quad (19)$$

260

261

262

263

264

265

266

267

268

269

270

271

272

Now we check the goodness of fit for the reduced-order model, that is, how well  $\hat{F}_{L_p}$  matches that of the full model,  $F_{L_p}$ . One calculates the maximum difference in the cumulative distribution functions,  $D_n$ , as in equation (20), and checks that satisfies inequality (21). To apply the two-sample Kolmogorov-Smirnov goodness-of-fit test at the 1% significance level, use  $c_{ks} = 1.63$ ; at the 5% significance level,  $c_{ks} = 1.36$ . It is also desirable to ensure that errors in the mean and coefficient of variation of  $L_p$ , defined by equations (22) and (23) respectively, are both less than some reasonable limit, say 5%; refer to inequalities (24) and (25). If the reduced model passes the test specified in equation (21), we can reject at the 1% significance level that the two distributions differ. If it fails equation (24), the reduced model is drifting too far in the mean, even if the Kolmogorov-Smirnov test says that it and the full model are still drawn from the same distribution. If it fails equation (25), the reduced model is (probably) getting too certain, even if the Kolmogorov-Smirnov test says it is drawn from the same distribution.

273

$$D_n = \max_l \left( \left| F_{L_p}(l) - \hat{F}_{L_p}(l) \right| \right) \quad (20)$$

274

$$D_n \leq c_{ks} \sqrt{\frac{z+Z}{z \cdot Z}} \quad (21)$$

275

$$\varepsilon_{\mu} = \frac{\hat{\mu}_{L_p} - \mu_{L_p}}{\mu_{L_p}} \quad (22)$$

276

$$\varepsilon_{\delta} = \frac{\hat{\delta}_{L_p} - \delta_{L_p}}{\delta_{L_p}} \quad (23)$$

277

$$|\varepsilon_{\mu}| \leq 0.05 \quad (24)$$

278

$$|\varepsilon_{\delta}| \leq 0.05 \quad (25)$$

279

280

**Path search.** With the foregoing equations, we can apply the path-search technique from Porter et al. (2017) to model order reduction for  $L_p$ .

281

1. Evaluate  $F_{L_p}(l)$ ,  $\mu_{L_p}$ , and  $\delta_{L_p}$  for the full model as shown in equations (1) through (13).

282

2. Let  $a$  denote an index to independent variables and  $b$  denote an index to their possible

283

values. For each  $(a, b)$  pair, fix variable  $a$  at value  $b$ . For each leaf  $j$ , calculate  $D_n$ ,  $\varepsilon_{\mu}$ , and

284  $\varepsilon_\delta$  from equations (20), (22), and (23), where  $I_j = 1$  if the leaf has variable  $a$  equal to value  
 285  $b$ , or  $I_j = 0$  if otherwise.

286 3. Trim the first branch ( $c = 0$ ) by selecting the  $(a, b)$  pair with the smallest value of  $D_n$  that  
 287 satisfies the goodness-of-fit test in inequality (21) and inequalities (24) and (25). Fix  
 288 variable  $a$  at value  $b$ . Variable  $a$  is no longer a free variable. One can say the model has  
 289 been reduced by variable  $a$ . Record the model size  $z$  of the model with one trimmed branch.

290 4. Trim the second branch ( $c = 1$ ) by repeating steps 2 and 3 starting with the reduced model  
 291 from step 3, but allowing every remaining  $(a, b)$  pair where  $a$  has not already been fixed.

292 5. Repeat until all branches are fixed ( $c = 2, 3, \dots, N_c - 1$ ) where  $N_c$  is the number of branches  
 293 in the logic tree.

294 **APPLICATION TO UCERF3-TD TREE TRIMMING PROBLEM**

295 *Independent variables: branches of UCERF3-TD plus three ground-motion branches.*

296 To estimate ground motion, we add three uncertainties not shown in Figure 1: site  
 297 characteristics (which model of Vs30—average shear-wave velocity in the upper 30 m of  
 298 soil—to use), which of five ground-motion-prediction equations to use, and how much  
 299 epistemic uncertainty to add. Note that Field et al. (2020) suggest that added epistemic  
 300 uncertainty is improperly posed and may exert a large, unjustified influence on results, but we  
 301 still included it here.

302 Table 1 summarizes the independent variables considered here: their type (scalars, denoted  
 303 by S, ordinals, denoted by O, and nominal, denoted by N), their possible values, weights (that  
 304 is, their conditional probabilities in a Bayesian sense), and a brief description. The description  
 305 explains to the reader who is unfamiliar with UCERF3-TD what each variable represents. The  
 306 description includes notes about how influential one might expect the variable to be on overall  
 307 uncertainty in rare portfolio loss. These notes are largely drawn from observations by Field et  
 308 al. (2013) on the influence each variable has on peak ground acceleration with 2% exceedance  
 309 probability in 50 years.

310 **Table 1.** Independent variables, variable types, possible values, weights, and descriptions

A	Variable (branch) name	Type	$b$	Possible value <sup>1</sup>	$w$	Description. See Field et al. (2013) Table 15 for maps of size and extent of effects.
0	Fault model	N	0	FM 3.1	0.5	Geometry of larger, more active faults. FM3.1 has 2,606 subsection and 253,706 multi-subsection ruptures; FM3.2, 2,665 and 305,709.
			1	FM 3.2	0.5	
1	Deformation model	N	0	Geol	0.3	Slip rates and related factors for each fault section; strain accumulation before fault rupture; energy released. Reflects approach to handling earthquake dynamics. Significant effects on 2%/50-year PGA ( $\pm 25\%$ ) over many large regions ( $\geq 200$ km). Geol and ZengBB are closer to UCERF3.3 average than others.
			1	ABM	0.1	
			2	NeoK	0.3	
			3	ZengBB	0.3	

A	Variable (branch) name	Type	b	Possible value <sup>1</sup>	w	Description. See Field et al. (2013) Table 15 for maps of size and extent of effects.
2	Scaling relationship	N	0	SHAW 09m	0.2	Relates earthquake magnitude to rupture surface area or to area and rupture aspect ratio (length divided by width). Also relates slip length to rupture length and width. Effects are modest ( $\pm 12\%$ ) but affects many large regions ( $\geq 200$ km). ELL B SQL and SHAW 09m closer to UCERF3.2 average 2%/50-year PGA than others.
			1	ELL B	0.2	
			2	H&B 08	0.2	
			3	ELL B SQL	0.2	
			4	SHAW CSD	0.2	
3	Slip along rupture	N	0	Tapered	0.5	Relates fault slip to location along rupture. Very little influence: modest effect ( $\pm 12\%$ ) in a few ( $\sim 5$ ) local ( $\leq 100$ km) areas.
			1	Boxcar	0.5	
4	Total $M > 5$ event rate $\text{yr}^{-1}$	S	0	6.5	0.1	Small ( $\pm 5\%$ ) effect throughout much of California, but mostly away from metro areas. 7.9 closest to UCERF3.3 average 2%/50-year PGA.
			1	7.9	0.6	
			2	9.6	0.3	
5	Maximum off-fault magnitude	S	0	7.3	0.1	Maximum magnitude of earthquakes away from mapped faults. Almost no noticeable influence on 2%/50-year PGA from any of the three models.
			1	7.6	0.8	
			2	7.9	0.1	
6	Off-fault spatl seism PDF	N	0	UCERF2	0.5	Depicts the spatial distribution of off-fault gridded seismicity. Significant ( $\pm 25\%$ ) influence throughout much of California, but mostly away from metro areas.
			1	UCERF3	0.5	
7	Earthquake probability model	N	0	Low COV	0.1	Estimates how ready each fault segment is to rupture given stress accumulation since last rupture. Probabilities are lower on faults with recent large earthquakes. Mid to high coefficient of variation (COV, aperiodicity) likely closer to average than the other, more extreme, options.
			1	Mid COV	0.4	
			2	High COV	0.3	
			3	Poisson	0.2	
8	Vs30 model	N	0	Wills (2015)	0.5	Average shear-wave velocity in upper 30 m of soil using correlation between observed Vs30 and geologic unit (Wills et al. 2015) or topographic slope (Wald and Allen 2007).
			1	Wald Allen (2007)	0.5	
9	Ground-motion-prediction equation	N	0	ASK2014	0.22	Relates ground motion (e.g., 5% damped spectral acceleration response) to magnitude, distance, fault attributes, and site conditions. BSSA2014 and CY2014 tend to be closer to the average of the four for common conditions in the middle distance (10-30 km) for a large ( $M 7.8$ ) earthquake on common site conditions ( $V_{s30} = 300$ m/sec, $D_{1.0} = 100$ m, $D_{2.5} = 1$ km). Significant ( $\pm 25\%$ ) influence statewide.
			1	BSSA2014	0.22	
			2	CB2014	0.22	
			3	CY2014	0.22	
			4	IDR2014	0.12	
10	Added epistemic uncertainty	S	0	Low	0.185	Adds ground motion uncertainty to account for collaboration among the NGAWest-2 developers and their use of common sets of statistical analyses and simulations to constrain parts of the models. Likely to have significant statewide effect.
			1	Med	0.630	
			2	High	0.185	

311 1. Abbreviations per Field et al. (2013)

312 Variables 0 through 7 are elements of UCERF3-TD. They represent  $2 \times 4 \times 5 \times 2 \times 3 \times 3$   
313  $\times 2 \times 4 = 5,760$  possible combinations. To calculate the repair cost to a portfolio of buildings  
314 requires additional variables 8 through 10, that is, variables that are exogenous to UCERF3-  
315 TD but endogenous to the (broader) loss model used here to trim the UCERF3-TD logic tree  
316 using losses. Variables 8, 9, and 10 have  $2 \times 5 \times 3 = 30$  possible combinations, for a total of  
317 172,800 model leaves when combined with the UCERF3-TD leaves. Of the 11 variables, four  
318 (numbers 4, 5, 7, and 10) involve scalar quantities and the others are nominal, that is, a choice  
319 among values with no order or scale. To calculate repair cost for a single scenario or for a loss  
320 exceedance curve also requires inputs that one could consider independent variables:

321 **Portfolio.** We considered a portfolio of buildings similar in composition, value, and  
322 geographic distribution to the one insured by the California Earthquake Authority, the state's  
323 largest insurer of earthquake risk to residences. The portfolio represents an estimate of the  
324 assets exposed to risk. Each asset is parameterized with its geographic location, site conditions  
325 ( $V_{s30}$ ), replacement cost new (the cost to build a new facility approximately functionally and  
326 aesthetically equivalent to the existing one), and a building type. "Building type" is often  
327 parameterized (as it is here) by structural material (e.g., wood), lateral force resisting system  
328 (e.g., shearwall), height category (e.g., 1-3 stories), and era of construction (e.g., pre-1940).

329 We estimated the inventory of woodframe single-family dwellings in California using a 2002-  
330 era database in Hazus-MH (Federal Emergency Management Agency 2012), factored up on a  
331 statewide basis to account for population growth and construction costs, and then factored  
332 down on a county-by-county basis to account for the California Earthquake Authority’s market  
333 penetration rate—that is, the fraction of homes they insure. We use a fixed value of the  
334 portfolio, rather than varying it. In the present case, the portfolio has an estimated replacement  
335 cost new of \$483 billion (2019 USD). Refer to the research data statement for the portfolio  
336 data.

337 ***Vulnerability functions.*** These relate ground motion to mean repair cost (and sometimes  
338 variability) as a fraction of replacement cost new. We used Hazus-based vulnerability functions  
339 from Porter (2009a, b, 2010). Vulnerability functions can be considered a variable that we  
340 fixed. Other models are available, but to vary the vulnerability functions seems relatively  
341 unimportant for the present objective of trimming the UCERF3-TD logic tree.

## 342 **RESULTS FOR LOSS $L$ WITH VARIOUS EXCEEDANCE PROBABILITIES**

343 Insurers commonly evaluate liquidity at the 1-in-250-year mark ( $p = 0.004$  per year)  
344 primarily because of rating agencies’ target and stress-test levels since the 2004/2005 hurricane  
345 seasons. That target assumes an insurer with several lines of business in several states, which  
346 provide diversification benefits. The California Earthquake Authority is different for exactly  
347 these reasons: one line of business, one state, all catastrophe risk. The California Earthquake  
348 Authority’s current risk-transfer strategy approved by its board (and revealed in the public  
349 domain) is to maintain a minimum of 1 in 400 and a maximum of 1 in 550-year claim-paying  
350 capacity (here,  $p = 0.0025$  to  $0.0018$ ). Therefore, we evaluate  $p \in \{0.01, 0.004, 0.0025, 0.0018,$   
351  $0.0004\}$ . Refer to Porter et al. (2024) for more details.

352 Table 2 summarizes results. Columns reflect probability levels. Rows show independent  
353 variables organized from least to most important. The least important can be trimmed from all  
354 models without significantly affecting the probability distribution of the dependent variable.  
355 Where a variable can be trimmed, the table shows the value to which it can be set. Some  
356 variables always strongly influence the dependent variable. Some only affect the dependent  
357 variable for some probabilities. The maximum off-fault earthquake magnitude can be set to 7.6  
358 in all cases. The fault model can also be fixed in all cases, but the preferred value is FM3.1 in  
359 some cases and FM3.2 in others. One variable, called “additional epistemic uncertainty” cannot

360 be trimmed at all without greatly disturbing the dependent variables. It seems improperly posed  
 361 and may exert an unjustified influence on results.

362 Table 2 shows that the optimal trimmed logic tree differs depending on exceedance  
 363 probability level. So how can one get value from it in practice? We suggest a pragmatic  
 364 approach: use the 1/250 choices regardless of the probability level of interest. Its choices share  
 365 parameter values most common to all five probability levels. It greatly reduces the  
 366 computational effort, but neither by the most nor the least, a sort of golden mean for model  
 367 order reduction. And 1/250 may be the most common point insurers and reinsurers consider on  
 368 the loss exceedance curve. However, this is just a suggestion; other opinions may differ.

369 Table 3 summarizes the size of each reduced-order model. Columns indicate the dependent  
 370 variable for which the model was trimmed. Rows show the size of the full and reduced models.

371 **Table 2.** Variables that can be trimmed from the logic tree and set to a deterministic value

Variable	Preferred value of trimmed variable for exceedance probability $p =$					EAL (app 4)
	1/100	1/250*	1/400	1/550	1/2500	
Maximum Off-Fault Magnitude	7.6	7.6	7.6	7.6	7.6	7.6
Fault Model	3.1	3.2	3.1	3.2	3.2	3.1
Total Mag 5 Rate		7.9	7.9	7.9	7.9	7.9
Earthquake Probability Model	Mid COV	Mid COV	High COV	Mid COV		
Vs30 Model		W2015	WA2008	W2015	W2015	
Slip Along Rupt Mod (Dsr)		Uniform	Uniform	Uniform	Uniform	
Deformation Model			Neokinema	Avg Block	Neokinema	ZengBB
Scaling Relationship			ELL B SQL	Shaw 09m		
Spatial Seismicity PDF			UCERF2	UCERF2		
Ground Motion Model						ASK2014
Added Epist Uncertainty						

372 \* We recommend using the 1/250 results in general for reasons explained in the text  
 373

374 **Table 3.** Summary of the degree of model order reduction

Model size		Repair cost $L_p$ with exceedance probability $p =$				
		1/100	1/250	1/400	1/550	1/2500
Full model	Independent variables	11	11	11	11	11
	Logic-tree leaves	172,800	172,800	172,800	172,800	172,800
Reduced order	Independent variables	8	5	2	2	5
	Logic-tree leaves	7,200	600	15	15	600
Reduced ÷ full	Independent variables	73%	45%	18%	18%	45%
	Logic-tree leaves	4%	0.3%	0.009%	0.009%	0.3%

375

376

## SUMMARY AND CONCLUSIONS

377 We identify a reduced-order model for the UCERF3-TD logic-tree model using a subset of  
 378 11 independent variables that reproduces the probability distribution of an important dependent  
 379 variable: loss at a low nonexceedance probability. We considered six dependent variables  
 380 related to the building repair cost for a statewide portfolio of buildings that approximates that  
 381 of the California Earthquake Authority's insurance portfolio of insured single-family

382 dwellings. The dependent variables are the total repair cost in a single earthquake with each of  
383 five exceedance probabilities, plus expected annualized loss.

384 Our model order reduction technique starts by evaluating the probability distribution of the  
385 full model's dependent variable. It trims one independent variable at a time, setting it to one  
386 possible value and tests whether the probability distribution of the dependent variable  
387 significantly changes or its first two moments significantly change relative to the full model.  
388 The reduced-order model with the smallest change is preferred. One iterates until reaching the  
389 smallest model that preserves the probability distribution of the dependent variable (passing a  
390 two-sample Kolmogorov-Smirnov test at 1% significance) and the dependent variable's first  
391 two moments within  $\pm 5\%$ . We applied the technique to the loss exceedance curve.

392 At loss-exceedance probabilities generally used by insurers and the California Earthquake  
393 Authority in particular (1/250 to 1/550), one can trim six to nine of UCERF3-TD's 11  
394 independent variables, reducing the model by 99.7% to 99.991%. We recommend fixing six  
395 parameters as shown in Table 2 for the California Earthquake Authority's 1/250-year loss.  
396 Doing so reduces the model size and computational effort by 99.7%. A hypothetical risk  
397 calculation that takes 24 hours for the full model can be reduced one that takes seconds.

398 This technique can handle a model that produces a scalar dependent variable that depends  
399 on scalar and nominal independent variables. It allows for interaction between independent  
400 variables. This is the first time this technique was applied to large, rare losses (points on the  
401 loss exceedance curve) in a large building portfolio. An earlier application of the technique  
402 only examined expected annualized loss. The technique worked as expected, since the  
403 problems differ mostly in the choice of the dependent variable. The technique reduced the loss  
404 model from 172,800 leaves to 15 leaves in the cases of the 400- and 550-year repair cost.

405 Which independent variables can be trimmed depends on the choice of dependent variable.  
406 The preferred value of the trimmed variables can also depend on which dependent variable one  
407 cares about. Only two variables cannot be trimmed from the logic tree for any of the dependent  
408 variables considered here: ground-motion-model additional epistemic uncertainty and ground  
409 motion model. With greater study of those two uncertainties, researchers might reduce them.  
410 Doing so would thin the upper tail of the loss distribution. It would save insurers on  
411 reinsurance. And it would save policyholders on premium costs that help pay for reinsurance.



412 With some limitations discussed next, the present model order reduction technique seems  
413 applicable to future earthquake rupture forecasts and other risk models that share the features  
414 of UCERF3-TD: a combination of independent (or transformable to independent) scalar and  
415 nominal uncertain variables, and probably ordinal variables as well.

416 All studies are limited. Good ones raise interesting questions. Here are some limitations  
417 and some questions. First, we applied the technique only to a single deterministic statewide  
418 portfolio. Would other portfolios have different results? We suspect they will be like the  
419 differences between columns in Table 2, sharing many common choices.

420 We did not account for uncertainty in the vulnerability functions. How important is that?  
421 Nor did we account for other uncertainties in the portfolio. For example, how important is  
422 uncertainty in the assignment of building type to individual assets, or uncertainty in asset  
423 replacement cost? Both  $EAL$  and  $L_p$  would scale linearly with an across-the-board under- or  
424 over-estimation of asset replacement cost, but the uncertainty might not work that way.

425 We did not consider the effects of spatiotemporal clustering (e.g., large damaging  
426 aftershocks), which can have a larger influence on expected annual losses than all the  
427 uncertainties considered here, as demonstrated by Field et al. (2017).

428 Can one identify *a priori* the branches of the complete logic-tree that contribute much less  
429 to the uncertainty than others, without first computing the losses for each combination?  
430 Tornado-diagram analysis examines the effect of each branch separately; it would be  
431 interesting to check whether the approach reliably predicts that the same variables matter.

432 Our method operates on one dependent variable. What if the model has more? Here are two  
433 options: (1) Produce a separate reduced-order model for each dependent variable, or (2) In step  
434 3 of the path search, calculate  $D_n$  for each dependent variable and trim branches by selecting  
435 the  $(a, b)$  pair with the smallest value of the *sum* of  $D_n$  values where *each individual*  $D_n$  satisfies  
436 the goodness-of-fit test in inequality (21) and inequalities (24) and (25).

## 437 **ACKNOWLEDGEMENTS AND DISCLAIMERS**

438 The California Earthquake Authority and the U.S. Geological Survey funded this work.  
439 The authors have no conflict of interest. Any use of trade, firm, or product names is for  
440 descriptive purposes only and does not imply endorsement by the U.S. Government. We thank  
441 reviewers E. Bilderback, J. Carter, R. Gold, K. Jaiswal, S.R. Kotha, and G. Weatherill.

442

## RESEARCH DATA AND CODE AVAILABILITY

443 Find the SA10 random fields at <https://doi.org/10.25810/xf0m-m080>, the building portfolio  
444 at <https://doi.org/10.25810/094s-mp33>, and OpenSHA code at <https://github.com/opensha/>.

445

## REFERENCES CITED

446 Abrahamson, N.A., Silva, W.J., and Kamai, R. (2014). Summary of the ASK14 ground motion relation  
447 for active crustal regions. *Earthquake Spectra* 30 (3): 1025-1055

448 Antoulas, A.C. (2005). Approximation of Large-Scale Dynamical Systems. Society of Industrial and  
449 Applied Mathematics, Philadelphia, 487 p.

450 Atik, L.A., and Youngs, R.R. (2014). Epistemic uncertainty for NGA-West2 models. *Earthquake*  
451 *Spectra* 30 (3), <https://doi.org/10.1193/062813EQS173M>

452 Awan, A.A. (2023). Intro to t-SNE. *DataCamp*. <https://www.datacamp.com/tutorial/introduction-t-sne>

453 Boore, D.M., Stewart, J.P., Seyhan, E., and Atkinson, G.M. (2014). NGA-West2 equations for  
454 predicting PGA, PGV, and 5% damped PSA for shallow crustal earthquakes. *Earthquake Spectra*  
455 30 (3): 1057-1085.

456 California Earthquake Authority (2022). *The Strength to Rebuild: Financial Foundations of the*  
457 *California Earthquake Authority*. Sacramento, CA

458 Chiou, B.S.J., and Youngs, R.R. (2014). Update of the Chiou and Youngs NGA model for the average  
459 horizontal component of peak ground motion and response spectra. *Earthquake Spectra*, 30(3):  
460 1117-1153.

461 Federal Emergency Management Agency (2012). *Multi-hazard Loss Estimation Methodology*  
462 *Earthquake Model Hazus®-MH 2.1 Technical Manual*. Washington, DC, 718 pp.

463 Field, E.H., Gupta, N., Gupta, V., Blanpied, M., Maechling, P., and Jordan, T.H. (2005). Hazard  
464 calculations for the WGCEP-2002 forecast using OpenSHA and distributed object technologies.  
465 *Seismological Research Letters* 76: 161-167.

466 Field, E.H., T.E. Dawson, K.R. Felzer, A.D. Frankel, V. Gupta, T.H. Jordan, T. Parsons, M.D. Petersen,  
467 R.S. Stein, R.J. Weldon II, and C.J. Wills, 2007. The Uniform California Earthquake Rupture  
468 Forecast, Version 2 (UCERF 2). U.S. Geological Survey Open File Report 2007-1437, Reston VA,  
469 96 p.

470 Field, E.H., Arrowsmith, R.J., Biasi, G.P., Bird, P., Dawson, T.E., Felzer, K.R., Jackson, D.D., Johnson,  
471 K.M., Jordan, T.H., Madden, C., Michael, A.J., Milner, K.R., Page, M.T., Parsons, T., Powers,  
472 P.M., Shaw, B.E., Thatcher, W.R., Weldon II, R.J., and Zeng, Y. (2013). Uniform California  
473 Earthquake Rupture Forecast, Version 3 (UCERF3)—the Time-Independent Model. U.S.  
474 Geological Survey Open-File Report 2013-1165, Reston VA, 115 p.

475 Field, E.H., Biasi, G.P., Bird, P., Dawson, T.E., Felzer, K.R., Jackson, D.D., Johnson, K.M., Jordan,  
476 T.H., Madden, C., Michael, A.J., Milner, K.R., Page, M.T., Parsons, T., Powers, P.M., Shaw, B.E.,  
477 Thatcher, W.R., Weldon II, R.J., and Zeng, Y. (2015). Long-term time-dependent probabilities for  
478 the third uniform California earthquake rupture forecast (UCERF3). *Bulletin of the Seismological*  
479 *Society of America*, 105 (2A): 1-33.

480 Field, E.H., Porter, K.A., and Miller, K.R. (2017). A prototype operational earthquake loss model for  
481 California based on UCERF3-ETAS – a first look at valuation. *Earthquake Spectra* 33 (4)

482 Field, E.H., Milner, K.R., and Porter, K.A. (2020). Assessing the value of removing earthquake-  
483 hazard-related epistemic uncertainties, exemplified using average annual loss in California.  
484 *Earthquake Spectra* 36 (4), <https://doi.org/10.1177/8755293020926185>

485 Jayaram, N., and Baker, J. (2009). Correlation model for spatially distributed ground-motion intensities.  
486 *Earthquake Engineering and Structural Dynamics* 38:1687-1708.

487 Loeve, M. (1955). *Probability Theory*. Van Nostrand Co Inc., New York, 516 pp.

488 McInnes, L., Healy, J., and Melville, J. (2020). *UMAP: Uniform Manifold Approximation and*  
489 *Projection for Dimension Reduction*. arXiv, <https://doi.org/10.48550/arXiv.1802.03426>

490 Perkins, D., and Taylor, C. (2003). Earthquake occurrence modeling for evaluating seismic risks to  
491 roadway systems. *Sixth U.S. Conference and Workshop on Lifeline Earthquake Engineering*  
492 *(TCLEE) 2003, August 10-13, 2003, Long Beach, California, United States*.  
493 [https://doi.org/10.1061/40687\(2003\)87](https://doi.org/10.1061/40687(2003)87)

494 Porter, K., Field, E., and Milner, K (2017). Trimming a hazard logic tree with a new model-order-  
495 reduction technique. *Earthquake Spectra*, 33(3): 857–874.

496 Porter, K.A. (2009a). Cracking an open safe: HAZUS vulnerability functions in terms of structure-  
497 independent spectral acceleration. *Earthquake Spectra* 25 (2): 361-378.

498 Porter, K.A. (2009b). Cracking an open safe: more HAZUS vulnerability functions in terms of  
499 structure-independent spectral acceleration. *Earthquake Spectra* 25 (3): 607-618.

500 Porter, K.A. (2010). Cracking an open safe: uncertainty in HAZUS-based seismic vulnerability  
501 functions. *Earthquake Spectra*, 26 (3): 893-900.

502 Porter, K.A., Field, E.H., and Milner, K. (2012). Trimming the UCERF2 hazard logic tree.  
503 *Seismological Research Letters*, 83 (5): 815-828.

504 Porter, K.A., Milner, K., and Field, E.H. (2024). Trimming the UCERF3-TD Logic Tree : Model Order  
505 Reduction for an Earthquake Rupture Forecast Considering Loss Exceedance, Supplemental  
506 Material. [CU Scholar...](#)

507 Prud'homme, C., Rovas, D.V., Veroy, K., Machiels, L., Maday, Y., Patera, A.T., and Turinici, G.  
508 (2002). Reliable real-time solution of parametrized partial differential equations: Reduced-basis  
509 output bound methods. *Journal of Fluids Engineering* 124(1): 70-80.

510 Schilders, W.H., Van der Vorst, H.A., and Rommes, J. (2008). *Model Order Reduction: Theory,*  
511 *Research Aspects and Applications*. Berlin: Springer, 471 p.

512 Shaw, B.E. (2009). Constant stress drop from small to great earthquakes in magnitude-area scaling,  
513 *Bulletin of the Seismological Society of America*, 99: 871.

514 Wald, D.J., and Allen, T.I. (2007). Topographic slope as a proxy for seismic site conditions and  
515 amplification. *Bulletin of the Seismological Society of America*, 97: 1379-1395.

516 Wills, C.J., Gutierrez, C.I., Perez, F.G., and Branum, D.M. (2015). A next generation VS30 map for  
517 California based on geology and topography. *Bull. Seism. Soc. of America* 105 (6): 3083–3091.

526